

Hydrodynamic Inverse Faraday Effect in Two Dimensional Electron Liquid

S. O. Potashin,¹ V. Yu. Kachorovskii,^{1,2,3} and M. S. Shur²

¹*Ioffe Institute, 194021 St. Petersburg, Russia*

²*Rensselaer Polytechnic Institute, 12180, Troy, NY, USA*

³*CENTERA Laboratories, Institute of High Pressure Physics, Polish Academy of Sciences, 01-142 Warsaw, Poland*

We show that a small conducting object, such as a nanosphere or a nanoring, embedded into or placed in the vicinity of the two-dimensional electron liquid (2DEL) and subjected to a circularly polarized electromagnetic radiation induces “twisted” plasmonic oscillations in the adjacent 2DEL. The oscillations are rectified due to the hydrodynamic nonlinearities leading to the helicity sensitive circular dc current and to a magnetic moment. This hydrodynamic Inverse Faraday Effect (HIFE) can be observed at room temperature in different 2D materials. The HIFE is dramatically enhanced in a periodic array of the nanospheres forming a resonant plasmonic coupler. Such a coupler exposed to a circularly polarized wave converts the entire 2DEL into a vortex state. Hence, the twisted plasmonic modes support resonant plasmonic-enhanced gate-tunable optical magnetization. Due to the interference of the plasmonic and Drude contributions, the resonances have an asymmetric Fano-like shape. These resonances present a signature of the 2DEL properties not affected by contacts and interconnects and, therefore, providing the most accurate information about the 2DEL properties. In particular, the widths of the resonances encode direct information about the momentum relaxation time and viscosity of the 2DEL.

I. INTRODUCTION

Generation of stationary magnetic moment by a circularly polarized radiation is commonly referred to as the inverse Faraday effect (IFE) predicted by Pitaevskii [1] and first observed by van der Ziel et al. [2]. Although this effect is usually studied in magnetic materials [3–5], it can be also observed in conventional semiconductor nanostructures such as quantum dots and nanorings [6–15]. In particular, it was recently predicted [14, 15] that a circularly polarized radiation with the electric component $\mathbf{E} = \mathbf{E}_\omega \exp(-i\omega t) + c.c.$ can excite a circular dc current in a nanoring, which, in turn, generates a magnetic moment

$$\mathbf{M} \propto i \mathbf{E}_\omega \times \mathbf{E}_\omega^*. \quad (1)$$

The proportionality coefficient in Eq. (1) is an odd function of frequency, so that the effect is sensitive to the helicity of polarization. Remarkably, IFE is dramatically enhanced in vicinity of plasmonic resonances [15]. Specifically, adjusting the plasmonic frequency in the

nanoring to match the frequency of impinging radiation results in much larger optically-induced stationary magnetic field (up to 0.1 Gauss for typical parameters of a nanoring, see discussion in Ref. [15]). Hence, an array of nearly identical quantum rings should give rise to large optically-controlled macroscopic magnetization. This opens a wide avenue for applications in tunable optoelectronics, in particular, in the terahertz (THz) range of frequencies.

The key feature of the plasmonic-enhanced IFE as compared to other plasma wave related effects is the absence of the symmetry limitations for conversion of incoming radiation into a dc signal. Indeed, in conventional plasmonic devices such conversion requires an asymmetry of the system that determines direction of the dc current. In the two-dimensional structures, the asymmetry can be created by the boundary conditions [16] or induced by ratchet effect (see Ref. 17 for review). The latter implies a special type of grating-gate couplers that could provide the required asymmetry. By contrast, IFE exists in fully symmetric rings [14, 15], and direction of arising dc current is simply determined

by the sign of circular polarization. What is also important in view of possible applications for the THz plasmonics, the optically-induced dc current remains finite even in the longwavelength limit, when \mathbf{E}_ω does not vary within the dimension of ring. Hence, the quantum nanorings and ring-based arrays can be used as an effective helicity-driven sensors for THz radiation [see estimates and discussion in Ref. [15]].

In this paper, we discuss the possibility of observing similar effects in bulk 2D systems. We consider the excitation of circular plasmonic modes (“twisted plasmons”) and circular dc current in two dimensional electronic liquid (2DEL). These modes are excited by a circularly polarized electromagnetic radiation impinging on the metallic or semiconducting nanosphere or nanoring embedded into or placed above the 2DEL and inducing rotating dipoles in these nanostructures (see Fig. 1a). Rectification of the twisted plasmons due to hydrodynamic nonlinearities leads to a helicity-sensitive circular DC current, and consequently, to a mag-

netic moment, thus demonstrating the hydrodynamic inverse Faraday effect (HIFE). If the nanospheres form a 2D crystal (see Fig. 1b), only the plasmons with the wave vectors forming inverse crystal lattice are excited, so that the excitation spectrum becomes discrete. When the radiation frequency is close to any of the discrete plasmonic frequencies, the entire high-mobility 2DEL experiences a resonant circular plasmonic excitation. The rectification of these oscillations leads to plasmonic-enhanced DC current which oscillates in space. The circular dc current and magnetic moment generated by this current show sharp HIFE resonances. Since the plasma wave frequency is tunable by the gate voltage and by an external magnetic field such a system can be used for optical tunable magnetization of 2D systems. The typical 2DEL twisted plasmon frequencies are in the THz range, and this coupling system could be used for tunable THz electronic components, including frequency multipliers, modulators, absorbers, and mixers. Another key application is in the contactless characterization and parameter extraction of the 2DEL.

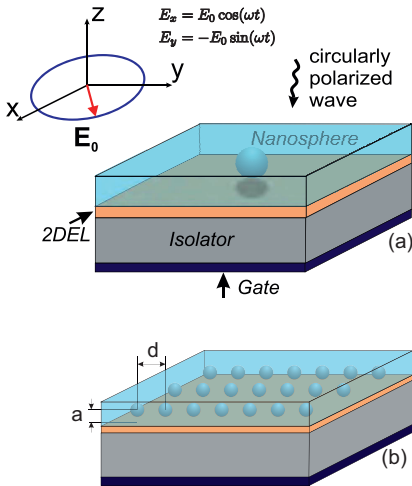


FIG. 1. Excitation of twisted plasmons in 2D electron liquid by a single nanosphere embedded into dielectric matrix and excited by circularly polarized radiation (a) or by an array of nanospheres forming plasmonic coupler (b)

Apart from applications, there are some very interesting fundamental aspects of the HIFE related to hydrodynamic approach in plasmonics, the field which explores how electromagnetic fields can be confined over dimensions much smaller than the radiation wavelength [18–24]. The hydrodynamic approach to description of electronic systems and, in particular, plasma wave excitation, has a long history which can be traced back to the early work by Gurzhi [25] and by Jong and Molenkamp [26], where hydrodynamic effects on the electron and phonon transport were discussed and to the work by Dyakonov and Shur [16], which exploited the analogy between the “shallow water” hydrodynamics and that of the electron liquid in the two-dimensional (2D) gated systems. Many other beautiful hydrodynamic phenomena such as choking of electron flow [27], nonlinear rectification of the plasma waves [28, 29] and the formation of the plasmonic shock waves [30] have been subsequently proposed. Possible applications of these phenomena to the plasma-wave

electronics were intensively discussed (see reviews [31, 32]). More recent interest to the hydrodynamic phenomena in low-dimensional transport and plasmonics is driven by the emergence of the high-mobility nanostructures [33–41] and graphene [42–52] where the electron-electron collision-dominated transport regime can be reached.

Two issues that have been most actively discussed in recent years are the emergence of hydrodynamic regimes with nonzero vorticity (and their manifestation in the transport properties of the 2DEL) (see [40, 48–52] and references therein), as well as possible methods for measuring the viscosity by using dynamical excitations of 2DEL [40], and by nonlocal resistance measurements [48–52].

Here, we demonstrate that the electron flow with nonzero vorticity can be also excited by circular polarized radiation. Importantly, we find that such states appear even in an ideal 2DEL with zero viscosity. We also find that the main effect of viscosity is broadening of the plasmonic resonances in the structure shown in Fig. 1b. Corresponding contribution to the resonance width is proportional to the kinematic viscosity and depends on the single geometrical factor—the distance between nanospheres a . This enables optical measurements of the electron liquid viscosity.

II. BASIC EQUATIONS

In this work, we propose to excite circular plasmon excitation (twisted plasmons) through the periodic array of metal objects (or semiconducting objects with high conductivity), such as nanospheres or nanorings, embedded into 2DEL or placed in the vicinity of the 2DEL by using insulating matrix transparent for THz radiation. To begin with, we consider the excitation of a single nanosphere (see Fig. 1 a), and then generalize the results to the case of the grating plasmonic coupler consisting of the periodic array of nanospheres (see Fig. 1 b).

Circularly polarized electromagnetic radiation induces a dipole potential in the

nanosphere. As a result, an inhomogeneous field is formed, which, in turn, acts on the 2DEL. We will find the dc response of the system. We assume that: (i) electron-electron collisions prevail over scattering by phonons and impurities; (ii) the radiation wavelength is much larger than the radius of the nanosphere, so that the electric field of radiation is uniform; (iii) the system is gated. First assumption allows us to use hydrodynamic approximation.

The 2D electron liquid is described by hydrodynamic equations for dimensionless electron concentration $n = (N - N_0)/N_0$ and velocity \mathbf{v} :

$$\frac{\partial n}{\partial t} + \text{div}[(1+n)\mathbf{v}] = 0, \quad (2)$$

$$\frac{\partial \mathbf{v}}{\partial t} + (\mathbf{v}\nabla)\mathbf{v} + \gamma\mathbf{v} + s^2\nabla n - \nu\Delta\mathbf{v} = \frac{e\mathbf{E}}{m}. \quad (3)$$

Here N_0 is equilibrium concentration, s is the plasma wave velocity, γ is the rate of the momentum relaxation, ω is the radiation frequency, m is the electron mass, and ν is the kinematic viscosity (for simplicity, we neglect the bulk contribution to viscosity). The field acting in the 2D plane, $\mathbf{E} = \mathbf{E}_0(t) + \mathbf{E}_1(t, \mathbf{r})$ is given by the sum of the homogeneous field of circularly polarized incoming radiation, $\mathbf{E}_0(t) = E_0(\cos\omega t, -\sin\omega t) = (E_0/2)(\mathbf{e}_x - i\mathbf{e}_y)\exp[-i\omega t] + c.c.$ and the dipole field

$$\mathbf{E}_1(\mathbf{r}, t) = -e\nabla \frac{\mathbf{r}\mathbf{p}(t)}{(r^2 + a^2)^{3/2}}, \quad (4)$$

where $\mathbf{p}(t) = p(\cos\omega t, -\sin\omega t)$ and $ep = E_0R^3$ is the dipole moment of a metallic nanosphere with radius R (we assume here that internal plasmonic frequency of the nanosphere is very large as compared to characteristic frequencies of the problem, so that its is fully polarized). For a lattice of the nanospheres, one should replace $\mathbf{E}_1(\mathbf{r}, t) \rightarrow \sum_i \mathbf{E}_1(\mathbf{r} - \mathbf{r}_i, t)$, where summation is taken over the lattice nodes.

The incoming radiation leads to the oscillations of the concentration and velocity, which are rectified due to the nonlinearity of the hydrodynamic equations. The small signal solution of hydrodynamic equations Eqs. (2) and

(3) can be found perturbatively by expansion over E_0 up to second order

$$n \approx \delta n(t, \mathbf{r}) + \bar{n}(\mathbf{r}), \quad \mathbf{v} \approx \delta \mathbf{v}(t, \mathbf{r}) + \bar{\mathbf{v}}(\mathbf{r}),$$

where $\delta n(t, \mathbf{r}) \propto E_0$ and $\delta \mathbf{v}(t, \mathbf{r}) \propto E_0$ are oscillations of the concentration and velocity representing linear response, and $\bar{n}(\mathbf{r}) \propto E_0^2$ and $\bar{\mathbf{v}}(\mathbf{r}) \propto E_0^2$ are time-independent corrections arising due to the rectification. We will see that the optically-induced flow of the 2DEL with nonzero vorticity appears even in ideal liquid with zero viscosity. Therefore, we will first put $\nu = 0$ and discuss viscosity related effects at the end of the paper. One of our main findings is that the finite viscosity leads to a very simple contribution to the width of plasmonic resonances. Hence, it can be extracted from experiments on the optical excitation of the plasmonic resonances.

A. Rectification of the optical signal

Next we demonstrate that radiation induces, due to the rectification, both a dc current \mathbf{j}_{dc} and a static electric potential ϕ_{dc} . To find the rectified corrections $\bar{n}(\mathbf{r})$ and $\bar{\mathbf{v}}(\mathbf{r})$ (squared-in- E_0) we average Eqs. (2) and (3) over time thus arriving at the following set of the stationary equations

$$\text{div} \bar{\mathbf{v}} = -\text{div} \mathbf{J}_1, \quad (5)$$

$$\gamma \bar{\mathbf{v}} + s^2 \nabla \bar{n} = \gamma \mathbf{J}_2 \quad (6)$$

with the rectified sources

$$\mathbf{J}_1 = \langle \delta n \delta \mathbf{v} \rangle_t, \quad \mathbf{J}_2 = -\frac{1}{\gamma} \langle (\delta \mathbf{v} \nabla) \delta \mathbf{v} \rangle_t. \quad (7)$$

To find total radiation-induced dc current, \mathbf{j}_{dc} , one should sum $\bar{\mathbf{v}}$ and the rectified source \mathbf{J}_1 . The radiation-induced potential, ϕ_{dc} which creates static electric field $E_{\text{dc}} = -\nabla \phi_{\text{dc}}$ is found from the condition $e \nabla \phi_{\text{dc}} / m = s^2 \nabla \bar{n}$. Thus, we have the following set of equations for \mathbf{j}_{dc} and ϕ_{dc} .

$$\mathbf{j}_{\text{dc}}(\mathbf{r}) = N_0 [\bar{\mathbf{v}}(\mathbf{r}) + \mathbf{J}_1(\mathbf{r})], \quad (8)$$

$$e \phi_{\text{dc}}(\mathbf{r}) = m s^2 \bar{n}(\mathbf{r}). \quad (9)$$

Hence, the key steps of the calculation are as follows. One should first linearize hydrodynamic equations (2) and (3) and find the linear response. The next step is to substitute thus found δn and $\delta \mathbf{v}$ into the expressions for the non-linear sources, given by Eq. (7), perform the time averaging and find $\mathbf{J}_{1,2}$. Then, one should calculate \bar{n} and $\bar{\mathbf{v}}$ by solving Eqs. (5), (6), and, finally, find \mathbf{j}_{dc} and ϕ_{dc} from Eqs. (8) and (9).

III. LINEAR RESPONSE: DRUDE AND PLASMONIC CONTRIBUTIONS

Since electric field entering r.h.s. of Eq. 3, has both homogeneous and inhomogeneous contributions, one can present oscillations of the velocity as a sum of the homogeneous Drude excitation and inhomogeneous dipole-induced plasmonic term, while

$$\delta \mathbf{v} = \delta \mathbf{v}^{\text{D}} + \delta \mathbf{v}^{\text{P}}. \quad (10)$$

Corrections to the concentration appear only due to the inhomogeneous perturbation, so that $\delta n = \delta n^{\text{P}}$. As we demonstrate below, the presence of two types of velocity excitations leads to interference effects, and, as a consequence, to the Fano-like asymmetry of the resonances.

Linearizing Eqs. (2) and (3) and writing $\delta n = \delta n_{\omega}(\mathbf{r}) e^{-i\omega t} + c.c.$, $\delta \mathbf{v} = \delta \mathbf{v}_{\omega}(\mathbf{r}) e^{-i\omega t} + c.c.$, after simple calculations (see Appendix A) we get

$$\delta n_{\omega}(\mathbf{r}) = \Delta Z(\mathbf{r}), \quad (11)$$

$$\delta \mathbf{v}_{\omega}(\mathbf{r}) = \underbrace{i\omega \nabla Z(\mathbf{r})}_{\delta \mathbf{v}_{\omega}^{\text{D}}} + \underbrace{\frac{eE_0(\mathbf{e}_x - i\mathbf{e}_y)}{2m(\gamma - i\omega)}}_{\delta \mathbf{v}_{\omega}^{\text{P}}}, \quad (12)$$

where, for the case of a single nanosphere

$$Z(\mathbf{r}) = -i2\pi l^2 \int \frac{d^2 q}{(2\pi)^2} \frac{e^{i\mathbf{q}\mathbf{r}} e^{-i\varphi_{\mathbf{q}}} e^{-qa}}{q^2 - k^2}. \quad (13)$$

Here $e^{-i\varphi_{\mathbf{q}}} = (q_x - iq_y)/q$,

$$l^2 = \frac{e^2 p}{2m s^2}, \quad (14)$$

and

$$k = \frac{\sqrt{\omega(\omega + i\gamma)}}{s} = k_0 + iQ. \quad (15)$$

The real and imaginary parts of k , respectively, k_0 and Q , have physical meaning of wave vector and spatial decrement of the optically excited plasma wave. In what follows, we assume $\gamma \ll \omega$. Hence, $k \approx (\omega + i\gamma/2)/s$, and, consequently, $k_0 \approx \omega/s$, $Q \approx \gamma/2s$. As seen, the spatial decrement of the wave is small

$$Q \ll k_0. \quad (16)$$

For the case of square dipole lattice with the lattice constant d , equation (13) is slightly modified by the replacement

$$\int \frac{d^2q}{(2\pi)^2} \rightarrow \frac{1}{d^2} \sum_{\mathbf{q}}$$

where wave vector \mathbf{q} runs over the inverse lattice vectors

$$\mathbf{q}_{nm} = \frac{2\pi}{d} (n\mathbf{e}_x + m\mathbf{e}_y) \quad (17)$$

Since velocity is given by the sum of two terms [see Eq. (10)], one can split both of the rectified sources $\mathbf{J}_{1,2}$ into two contributions—the plasmonic contribution and the mixed (plasmonic+Drude) contribution:

$$\mathbf{J}_i = \mathbf{J}_i^{\text{P}} + \mathbf{J}_i^{\text{M}} \quad (i = 1, 2),$$

where

$$\begin{aligned} \mathbf{J}_1^{\text{P}} &= \langle \delta n^{\text{P}} \delta \mathbf{v}^{\text{P}} \rangle_t, \quad \mathbf{J}_2^{\text{P}} = -\frac{\langle (\delta \mathbf{v}^{\text{P}} \nabla) \delta \mathbf{v}^{\text{P}} \rangle_t}{\gamma}, \\ \mathbf{J}_1^{\text{M}} &= \langle \delta n^{\text{P}} \delta \mathbf{v}^{\text{D}} \rangle_t, \quad \mathbf{J}_2^{\text{M}} = -\frac{\langle (\delta \mathbf{v}^{\text{D}} \nabla) \delta \mathbf{v}^{\text{P}} \rangle_t}{\gamma}, \end{aligned} \quad (18)$$

Equations Eq. (13) and (18) allow us to clarify basic physics issues in more detail. First of all, as seen, the integral in the r.h.s. of Eq. (13) contains a pole in the denominator, which reflects the plasmonic resonance occurring when ω is equal to the frequency of plasma wave with the wave vector q . However, the pole is smeared

out due to the integration over \mathbf{q} . The situation is different for a dipole lattice when integration should be replaced with summation. For small γ , the contributions of the different terms in the sum are well separated and can give sharp plasmonic resonances. The resonance condition,

$$\omega = \omega_{nm} = (2\pi s/d) \sqrt{n^2 + m^2}, \quad (19)$$

is satisfied for several pairs (n, m) . For example, resonance with the fundamental frequency

$$\omega_0 = \frac{2\pi s}{d}, \quad (20)$$

is given by sum over 4 pairs $(1, 0), (-1, 0), (0, 1)$ and $(0, -1)$ yielding

$$Z_0(\mathbf{r}) \propto \frac{1}{\omega_0^2 - \omega^2 - i\omega\gamma}, \quad (21)$$

with the frequency-independent coefficient of proportionality. Then, rectified dc currents has resonance dependence $\mathbf{J}_i^{\text{P}} \propto |Z(\mathbf{r})|^2$, $\mathbf{J}_i^{\text{M}} \propto Z(\mathbf{r})$. As a result, in vicinity of resonance, the expression for the circular dc current can be approximately presented as follows

$$\mathbf{j}_{dc} \approx \frac{\boldsymbol{\pi}(\mathbf{r})}{\Omega^2 + \Gamma^2/4} + \left[\frac{\boldsymbol{\mu}(\mathbf{r})}{\Omega + i\Gamma/2} + c.c. \right]. \quad (22)$$

where

$$\Omega = \frac{\omega - \omega_0}{\omega_0}, \quad \Gamma = \frac{\gamma}{\omega_0}, \quad (23)$$

are, respectively, dimensionless detuning and damping of the fundamental resonance, while terms proportional to dimensionless vectors $\boldsymbol{\pi}(\mathbf{r})$ and $\boldsymbol{\mu}(\mathbf{r})$ represent plasmonic and mixed contributions, respectively [exact expressions for these coefficients will be given below, see Eqs. (39), and (40) below]. Due to the interference of these terms, the resonance in \mathbf{j}_{dc} and ϕ_{dc} , has an asymmetric Fano-like shape. Interestingly enough, the degree of asymmetry depends on the coordinate \mathbf{r} .

An important comment is related to the radiation-induced vorticity of the 2DEL. On the formal level, function $Z(\mathbf{r})$ is a Green's function of hydrodynamic equations describing the

plasmonic excitation caused by a point-like rotating dipole. Due to this rotation, an angular moment ± 1 is transferred to the liquid with the sign determined by the sign of the helicity. The information about this moment is encoded in the phase factor $\exp[-i\varphi_{\mathbf{q}}]$ in Eq. (13). This means that the plasma waves circulate around the nanospheres and that direction of circulation changes with changing the sign of the radiation polarization. We call such excitations “twisted plasmons”. The rectification of these plasmons leads to dc current with non-zero vorticity, which is also determined by the helicity sign.

IV. CIRCULAR DC CURRENT INDUCED BY A SINGLE DIPOLE

Performing integration over $\varphi_{\mathbf{q}}$ in Eq. (13), we get

$$Z(\mathbf{r}) = l^2(x - iy)f(r), \quad (24)$$

where function f depends only on $r = |\mathbf{r}|$. The analytical expressions for f and its asymptotes are presented in the Appendix A together with expression of δn_{ω} and δv_{ω} in terms of f . It is convenient to present \mathbf{J}_i as follows

$$\mathbf{J}_i = R_i \mathbf{e}_{\mathbf{r}} + \Phi_i \mathbf{e}_{\phi}, \quad (25)$$

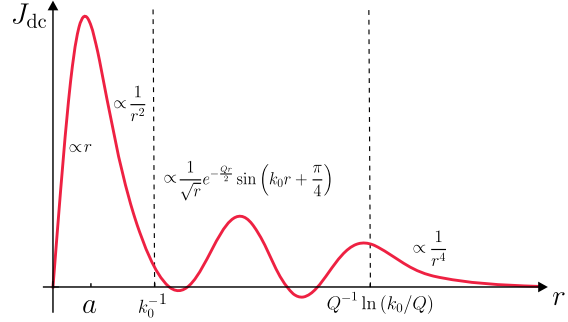


FIG. 2. Dependence of the circular current j_{dc} created in 2D liquid by a rotating dipole moment of a single nanosphere. Main contribution to this current comes from mixed term [See Eq. (28)]

where $\mathbf{e}_{\mathbf{r}} = \mathbf{r}/r$, $\mathbf{e}_{\phi} = \mathbf{e}_z \times \mathbf{e}_{\mathbf{r}}$, and functions $R_i = R_i^{\text{P}} + R_i^{\text{M}}$, and $\Phi_i = \Phi_i^{\text{P}} + \Phi_i^{\text{M}}$, depend only on $r = |\mathbf{r}|$ and contain both plasmonic and mixed contributions.

Provided that R_i and Φ_i are known, the solution of Eqs. (5) and (6) can be found by expanding $\bar{\mathbf{v}}$ over $\mathbf{e}_{\mathbf{r}}$ and \mathbf{e}_{ϕ} and assuming $\bar{n} = \bar{n}(r)$. We find for the total circular radiation-induced dc current, $\mathbf{j}_{\text{dc}} = j_{\text{dc}} \mathbf{e}_{\phi}$ and radial electric field, $E_{\text{dc}} = E_{\text{dc}} \mathbf{e}_{\mathbf{r}}$:

$$j_{\text{dc}} = N_0(\Phi_1 + \Phi_2) \quad (26)$$

$$\frac{eE_{\text{dc}}}{m} = \gamma(R_1 + R_2) \quad (27)$$

Expressions for plasmonic and mixed contributions, R_i^{P} , Φ_i^{P} and R_i^{M} , Φ_i^{M} , are presented in Appendixes B and C, respectively, as well as expressions for asymptotical behavior of j_{dc} [see Eq. (D1)] and E_{dc} [see Eq. (D2)] with account of both plasmonic and mixed contribution. As seen, for the most realistic case ($R \ll a \ll k_0^{-1} \ll Q^{-1}$), the mixed contribution dominates. Neglecting plasmonic contribution, we find that

$$j_{\text{dc}} \approx -j_* \begin{cases} C\left(\frac{r}{a}\right), & r \ll 1/k_0, \\ \frac{\sqrt{2\pi}k_0^{3/2}a^2}{\sqrt{r}}e^{-Qr/2}\sin(k_0r + \pi/4), & 1/k_0 \ll r \ll \frac{\ln[k_0/Q]}{Q}, \\ \frac{6a^2}{k_0^2r^2}, & \frac{\ln[k_0/Q]}{Q} \ll r \end{cases} \quad (28)$$

where

$$j_* = \frac{\omega l^4 N_0}{k_0^2 R^3 a^2}, \quad (29)$$

and $C(x)$ is given by Eq. (D4). Static optically-induced field is connected with the dc circular current by a simple relation

$$j_{\text{dc}} = -\frac{eE_{\text{dc}}N_0}{m\omega}. \quad (30)$$

A. Dipole lattice

For a lattice of dipoles, we write Fourier components of nonlinear sources \mathbf{J}_1 and \mathbf{J}_2 as follows

$$\mathbf{J}_{i\mathbf{q}\omega} = R_{i\mathbf{q}} \mathbf{n}_{\mathbf{q}}^{\parallel} + \Phi_{i\mathbf{q}} \mathbf{n}_{\mathbf{q}}^{\perp}, \quad i = (1, 2) \quad (31)$$

where $\mathbf{n}_{\mathbf{q}}^{\parallel} = \mathbf{q}/q$ and $\mathbf{n}_{\mathbf{q}}^{\perp} = \mathbf{e}_z \times \mathbf{q}/q$. The Fourier transform of Eqs. (5) and (6) yields expressions similar to Eqs. (26) and Eq. (27):

$$\mathbf{j}_{\mathbf{q}}^{\text{dc}} = N_0(\Phi_{1\mathbf{q}} + \Phi_{2\mathbf{q}})\mathbf{n}_{\mathbf{q}}^{\perp}, \quad (32)$$

$$\frac{e\mathbf{E}_{\mathbf{q}}^{\text{dc}}}{m} = \gamma(R_{1\mathbf{q}} + R_{2\mathbf{q}})\mathbf{n}_{\mathbf{q}}^{\parallel}. \quad (33)$$

The Fourier components of the dc current and static field can be presented as sums over plasmonic and mixed contributions: $R_{i\mathbf{q}} = R_{i\mathbf{q}}^{\text{P}} + R_{i\mathbf{q}}^{\text{M}}$, $\Phi_{i\mathbf{q}} = \Phi_{i\mathbf{q}}^{\text{P}} + \Phi_{i\mathbf{q}}^{\text{M}}$.

We consider simplest case of a square lattice with the lattice constant d . In this case, all the integrals over \mathbf{q} should be replaced with the sums over the vectors of the inverse lattice [see

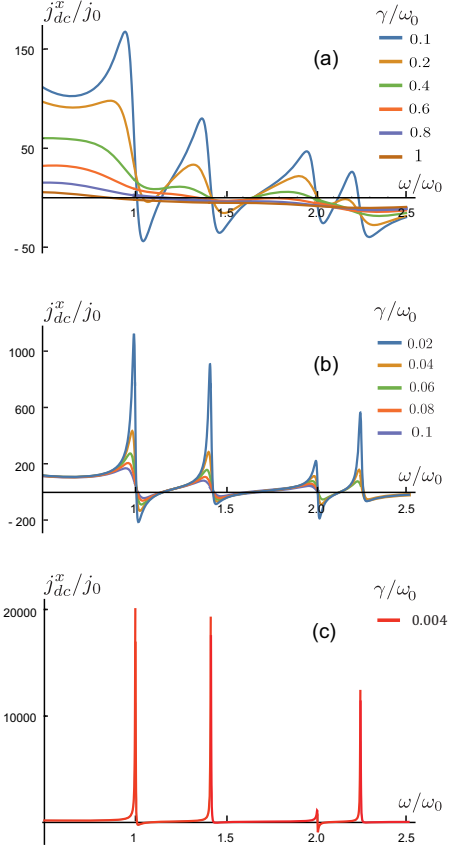


FIG. 3. Frequency dependence of x -component of the current for $x = y = d/8$, $R = a/2$, $d = 5a$: onset of plasmonic resonances at large γ (a); strongly asymmetric resonances at intermediate values of γ (b); weakly asymmetric resonances at very small γ (c).

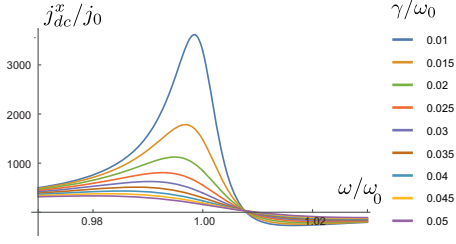


FIG. 4. Fundamental plasmonic peak in x component of dc current for $x = y = d/8$, $R = a/2$, $d = 5a$ and different values of γ . The asymmetry of the peak decreases with decreasing of γ .

Eq. (17)] and function $Z(\mathbf{r})$ becomes

$$Z(\mathbf{r}) = -\frac{i2\pi l^2}{d^2} \sum_{\mathbf{q}} \frac{e^{i\mathbf{q}\mathbf{r}}}{q^2 - k^2} e^{-i\varphi_{\mathbf{q}}} e^{-q a}. \quad (34)$$

Using this equation, we find

$$\delta n_{\omega} = \frac{2i\pi l^2}{d^2} \sum_{\mathbf{q}} \frac{e^{i\mathbf{q}\mathbf{r}} e^{-i\varphi_{\mathbf{q}}} q^2 e^{-q a}}{q^2 - k^2}, \quad (35)$$

$$\delta \mathbf{v}_{\omega} = \frac{2i\pi l^2}{d^2} \sum_{\mathbf{q}} \frac{e^{i\mathbf{q}\mathbf{r}} e^{-i\varphi_{\mathbf{q}}} \omega \mathbf{q} e^{-q a}}{q^2 - k^2} + \frac{eE_0(\mathbf{e}_x - i\mathbf{e}_y)}{2m(\gamma - i\omega)}. \quad (36)$$

The rectified currents $\mathbf{J}_i^{\text{P,M}}$ can be calculated using Eqs. (18), (35), and (36). Corresponding analytical expressions are given in Appendix E. Resulting equations for \mathbf{j}_{dc} and \mathbf{E}_{dc} are given, respectively, by Eqs. (E5) and (E6).

In Fig. 3 we plotted the x -component of the dc current in units of

$$j_0 = N_0 \frac{4\pi^2 l^4 s}{d^4},$$

in a certain point in the plane as a function of the radiation frequency for different damping rates (picture for the y component of the current looks analogous). As seen, with decreasing the γ , sharp resonances appear on the top of the smooth dependence. Due to the interference of

the plasmonic and mixed contributions, the resonances have an asymmetric shape. The degree of asymmetry is smaller for small γ , because the symmetric plasmonic contribution dominates at $\gamma \rightarrow 0$. Fig. 4 illustrates the asymmetry of the peaks for fundamental mode. To demonstrate vorticity of the current, we also plotted the calculated current vector density in Fig. 5.

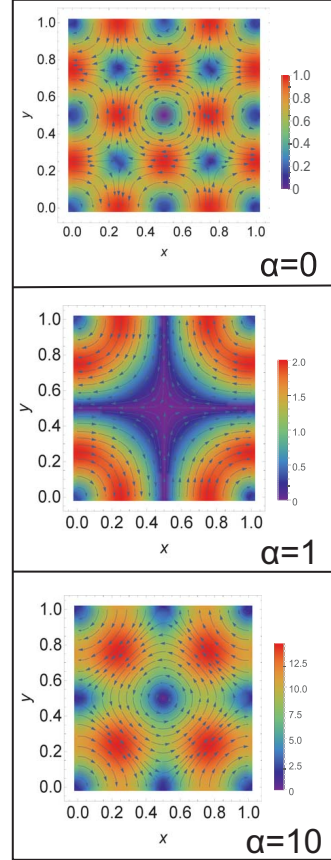


FIG. 5. Vector density plot of the rectified current \mathbf{j}_{dc} for different values of parameter $\alpha = 2\Omega\mu_0/\pi_0$.

B. Excitation of the fundamental mode

The smallest frequency, where the resonance can occur, is given by Eq. (20). For

ω close to ω_0 , within the resonance approximation, only four terms, with $(n, m) = (1, 0), (0, 1), (-1, 0), (0, -1)$, contribute to sum over \mathbf{q}_{nm} . For all these terms we have $q = q_0 = 2\pi/d$. Concentration and velocity look

$$\delta n_\omega = \frac{4\pi l^2}{d^2} \frac{q_0^2 e^{-q_0 a} [i \sin(q_0 y) - \sin(q_0 x)]}{q_0^2 - k^2}, \quad (37)$$

$$\begin{aligned} \delta \mathbf{v}_\omega = & \frac{4\pi l^2}{d^2} \frac{\omega \mathbf{q}_0 e^{-q_0 a} [i \mathbf{e}_x \cos(q_0 x) + \mathbf{e}_y \cos(q_0 y)]}{q_0^2 - k^2} \\ & + \frac{e E_0 (\mathbf{e}_x - i \mathbf{e}_y)}{2m(\gamma - i\omega)}, \end{aligned} \quad (38)$$

Using equations given in Appendix F, we find that the circular current can be presented in the form of Eq. (22), with

$$\begin{aligned} \boldsymbol{\pi}(\mathbf{r}) = & \pi_0 [\sin(q_0 y) \cos(q_0 x) \mathbf{e}_x \\ & - \sin(q_0 x) \cos(q_0 y) \mathbf{e}_y], \end{aligned} \quad (39)$$

$$\boldsymbol{\mu}(\mathbf{r}) = \mu_0 [\sin(q_0 y) \mathbf{e}_x - \sin(q_0 x) \mathbf{e}_y], \quad (40)$$

where

$$\pi_0 = \frac{8\pi^2 N_0 s l^4}{d^4} e^{-2q_0 a}, \quad \mu_0 = \frac{N_0 s l^4}{d R^3} e^{-q_0 a} \quad (41)$$

As seen, $\text{div} \boldsymbol{\pi} = \text{div} \boldsymbol{\mu} = 0$, so that \mathbf{j}_{dc} is purely circular current, $\text{div} \mathbf{j}_{\text{dc}} = 0$, with non-zero vorticity:

$$\begin{aligned} \nabla \times \mathbf{j}_{\text{dc}} = & -\mathbf{e}_z \frac{2q_0}{\Omega^2 + \Gamma^2/4} \\ & \times \{ \pi_0 \cos(q_0 x) \cos(q_0 y) \\ & + \mu_0 \Omega [\cos(q_0 x) + \cos(q_0 y)] \}. \end{aligned} \quad (42)$$

Two interfering contributions, plasmonic and mixed, have different frequency dependencies in the vicinity of the resonance, symmetric and asymmetric ones, respectively. Interestingly, the degree of asymmetry depends on coordinate. For example, at line $\cos(q_0 x) + \cos(q_0 y) = 0$ the vorticity is symmetric function of Ω , while for $\cos(q_0 x) = 0$ or $\cos(q_0 y) = 0$, the vorticity is described by asymmetric mixed term. Vector density plot of the rectified current j_{dc} is plotted in Fig. 5 for different values of parameter

$$\alpha = \frac{2\Omega\mu_0}{\pi_0} = \frac{d^3\Omega}{4\pi^2 R^3} e^{q_0 a}, \quad (43)$$

which depends on dimensionless deviation from the resonance, Ω . Hence, changing radiation frequency, one can qualitatively change spatial distribution of dc current.

Analogously, one can calculate optically-induced static potential

$$\begin{aligned} \frac{e\phi_{\text{dc}}}{m} = & \frac{2\pi^2 l^4 s^2}{d^4} \frac{e^{-2q_0 a}}{\Omega^2 + \Gamma^2/4} \\ & \times \{ \cos(2q_0 x) + \cos(2q_0 y) \\ & - 4\alpha [\cos(q_0 x) + \cos(q_0 y)] \}. \end{aligned} \quad (44)$$

C. Optically-induced magnetic field

The stationary magnetic field induced by radiation obeys

$$[\nabla \times \mathbf{H}] = \frac{4\pi \mathbf{j}_{\text{dc}}(\mathbf{r})}{c} \delta(z). \quad (45)$$

Substituting $\mathbf{H} = [\nabla \times \mathbf{A}]$ ($\text{div} \mathbf{A} = 0$), making Fourier transform over \mathbf{r} , we find

$$k^2 \mathbf{A}_{\mathbf{k}} - \frac{d^2 \mathbf{A}_{\mathbf{k}}}{dz^2} = \frac{4\pi \mathbf{j}_{\text{dc}}^{\mathbf{k}}}{c} \delta(z). \quad (46)$$

Finite at $|z| \rightarrow \infty$ solution of this equation reads $\mathbf{A}_{\mathbf{k}}(z) = (2\pi/c k) \mathbf{j}_{\text{dc}}^{\mathbf{k}} \exp(-k|z|)$. Hence, the Fourier transform of the vector potential (and, consequently, of the magnetic field) is proportional to the Fourier transform of the dc current. In the vicinity of plasmonic peaks, only several \mathbf{k} satisfying resonant conditions contribute to the current and magnetic field, so that spatial dependence of the field is found by the summation over these discrete set of \mathbf{k} .

Let us, for example, calculate the perpendicular component of the field, H_z , in the fundamental mode within the resonance approximation. In this case, \mathbf{k} runs over $(\pm q_0, \pm q_0)$ for the plasmonic contribution and over $(\pm q_0, 0)$ and $(0, \pm q_0)$ for the mixed contribution [see Eqs. (39) and (40)]. Instead of summation over these \mathbf{k} , one can take into account that all terms in $\boldsymbol{\pi}(\mathbf{r})$ and $\boldsymbol{\mu}(\mathbf{r})$ are eigenfunctions of the Laplace operator and present the field in the operator form

$$H_z(\mathbf{r}, z) = \frac{e^{-\sqrt{-\Delta}|z|}}{\sqrt{-\Delta}} \frac{2\pi \mathbf{e}_z [\nabla \times \mathbf{j}_{\text{dc}}(\mathbf{r})]}{c}. \quad (47)$$

From this equation and Eq. (48), we find

$$H_z(\mathbf{r}, z) = -\frac{4\pi}{c} \frac{1}{\Omega^2 + \Gamma^2/4} \quad (48)$$

$$\times \left\{ \pi_0 \cos(q_0 x) \cos(q_0 y) \frac{e^{-\sqrt{2}q_0|z|}}{\sqrt{2}} \right.$$

$$\left. + \mu_0 \Omega [\cos(q_0 x) + \cos(q_0 y)] e^{-\sqrt{q_0}|z|} \right\}.$$

Density plot of the magnetic plot in the 2DEL plane, $H_z(\mathbf{r}, 0)$, is plotted in Fig. (6).

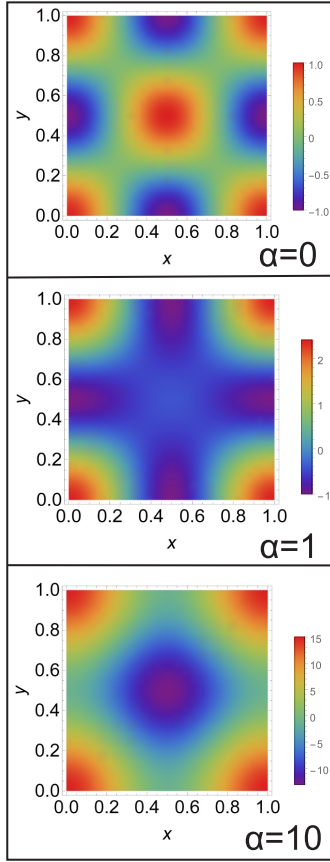


FIG. 6. Density plot of $H_z(\mathbf{r}, 0)$ for different values of parameter $\alpha = 2\Omega\mu_0/\pi_0$.

V. EFFECTS OF FINITE VISCOSITY AND EXTERNAL MAGNETIC FIELD

Above, we presented calculations at zero magnetic field for an ideal 2DEL with zero viscosity. The detailed analysis of different magnetoresponse regimes of the viscous electron liquid in the system under discussion is out of scope of this work and will be presented elsewhere. Here, we limit ourselves to the simplest but at the same time the most interesting case of the resonant excitation, when some of the plasmonic modes with wavevectors given by Eq. (17) satisfy the resonance condition: $\omega \approx \omega_{nm}$, where ω_{nm} is given by Eq. (19). In this case, within the resonant approximation, the effect of the weak magnetic field, B , with $\omega_c \ll \omega$ ($\omega_c = eB/mc$ is the cyclotron frequency) can be accounted by the replacement of ω_{nm}^2 with

$$\omega_{nm}^2(B) = \omega_{nm}^2 + \omega_c^2. \quad (49)$$

Hence, a weak magnetic field shifts positions of the resonances shown in Fig. 3 thus giving an additional way to control the dc current and magnetization.

Within the same resonance approximation, the effect of weak viscosity, satisfying the inequality $\nu q_{nm}^2 \ll \omega$, is accounted by replacement of elastic damping γ with

$$\gamma_{nm} = \gamma + \nu q_{nm}^2. \quad (50)$$

The resonance is described by Eq. (22) with

$$\Omega \approx \frac{\omega - \omega_{nm}(B)}{\omega_{nm}(B)}, \quad \Gamma \approx \frac{\gamma_{nm}}{\omega_{nm}}. \quad (51)$$

As seen from Eq. (50), measurement of widths of two plasmonic resonances with different resonance frequencies ($\omega_{n_1 m_1} \neq \omega_{n_2 m_2}$) allows one to extract value of ν :

$$\nu = \frac{(\gamma_{n_1 m_1} - \gamma_{n_2 m_2})d^2}{(2\pi)^2(n_1^2 + m_1^2 - n_2^2 - m_2^2)}. \quad (52)$$

Evidently, one can also extract momentum relaxation time by measuring $\gamma_{n_1 m_1}$ and $\gamma_{n_2 m_2}$. It worth noting that Eq. (52) does not include any characteristic of the material and depends on a

single geometrical factor—the distance between nanospheres, which can be well controlled in experiment. Hence, the HIFE gives a direct way to extract the electron viscosity.

VI. CONCLUSION

To conclude, we analyzed excitation of circular plasmonic modes (twisted plasmons) and circular dc current in two dimensional (2D) systems by circularly-polarized electromagnetic wave via a plasmonic coupler made of periodically placed nanospheres. We demonstrated that rectification of the plasma waves leads to a helicity-sensitive circular DC current, and consequently, to a magnetic moment, thus demonstrating the hydrodynamic inverse Faraday effect. The effect is dramatically increased in vicinity of plasmonic resonances, so that the DC current shows sharp plasmonic peaks. There are two interfering contributions to this peak, the plasmonic contribution, and the contribution involving both the plasmonic and the Drude excitations. As a result, plasmonic resonances have asymmetric Fano-like shape. The suggested system can be used for optical tunable magnetization of 2D systems, for many optoelectronic devices operating in the THz range of frequencies, and for the characterization and parameter extraction of 2DELs. In particular, measuring of the widths of different plasmonic resonances allows one to extract the electron viscosity.

VII. ACKNOWLEDGEMENT

The work of V.Yu.K. was supported by RFBR (Grant No. 20-02-00490), by Foundation for the Advancement of Theoretical Physics and Mathematics BASIS, and by the Foundation for Polish Science through the Grant No. MAB/2018/9 for CENTERA. The work at RPI was supported by the U.S. Army Research Laboratory Cooperative Research Agreement (Project Monitor Dr. Meredith Reed) and by the US ONR (Project Monitor Dr. Paul

Maki).

Appendix A: Linear response (technical details)

Linearizing Eqs. (2) and (3) and making Fourier transform we get

$$-i\omega\delta n_{\omega\mathbf{q}} + i\mathbf{q}\delta\mathbf{v}_{\omega\mathbf{q}} = 0, \quad (\text{A1})$$

$$i\mathbf{q}s^2\delta n_{\omega\mathbf{q}} + (\gamma - i\omega)\delta\mathbf{v}_{\omega\mathbf{q}} = \frac{\epsilon(\mathbf{E}_0 + \mathbf{E}_1)_{\omega\mathbf{q}}}{m}, \quad (\text{A2})$$

where

$$\left(\frac{\epsilon\mathbf{E}_0}{m}\right)_{\omega\mathbf{q}} = \frac{\epsilon E_0}{2m}(\mathbf{e}_x - i\mathbf{e}_y)(2\pi)^2\delta(\mathbf{q}) \quad (\text{A3})$$

$$\left(\frac{\epsilon\mathbf{E}_1}{m}\right)_{\omega\mathbf{q}} = -\frac{\pi\mathbf{q}e^2p}{m}e^{-i\varphi_{\mathbf{q}}}e^{-qa} \quad (\text{A4})$$

and $e^{-i\varphi_{\mathbf{q}}} = (q_x - iq_y)/q$

Solution of Eqs. (A1), (A2) reads

$$\delta n_{\omega\mathbf{q}} = 2\pi il^2 \frac{q^2}{q^2 - k^2} e^{-i\varphi_{\mathbf{q}}} e^{-qa}, \quad (\text{A5})$$

$$\delta\mathbf{v}_{\omega\mathbf{q}} = 2\pi il^2 \frac{\omega\mathbf{q}}{q^2 - k^2} e^{-i\varphi_{\mathbf{q}}} e^{-qa} + \frac{\epsilon E_0(\mathbf{e}_x - i\mathbf{e}_y)}{2m(\gamma - i\omega)} (2\pi)^2\delta(\mathbf{q}), \quad (\text{A6})$$

where l and k are given by Eqs. (14) and (15) of the main text. Next, we find Fourier transform of the velocity and concentration:

$$\delta n_{\omega}(\mathbf{r}) = \Delta Z(\mathbf{r}), \quad (\text{A7})$$

$$\delta\mathbf{v}_{\omega}(\mathbf{r}) = i\omega\nabla Z(\mathbf{r}) + \frac{\epsilon E_0(\mathbf{e}_x - i\mathbf{e}_y)}{2m(\gamma - i\omega)}, \quad (\text{A8})$$

where

$$Z(\mathbf{r}) = -i2\pi l^2 \int \frac{d^2q}{(2\pi)^2} \frac{e^{i\mathbf{q}\mathbf{r}} e^{-i\varphi_{\mathbf{q}}} e^{-qa}}{q^2 - k^2} = l^2(x - iy)f(r). \quad (\text{A9})$$

Function $f(r)$ is given by

$$f(r) = \int_0^\infty \frac{dq q J_1(qr) e^{-qa}}{r(q^2 - k^2)} \approx \frac{\pi}{2r} [\mathbb{H}_{-1}(kr) + iJ_1(kr)] - \frac{1}{r} \left(1 - \frac{r}{a + \sqrt{a^2 + r^2}}\right), \quad (\text{A10})$$

where \mathbb{H}_{-1} and J_1 are the Struve and Bessel functions. Here we assumed $Q \ll k_0 \ll 1/a$

[53].

Asymptotes of the function f are given by

$$f \approx \begin{cases} \sqrt{\frac{\pi}{2kr^3}} e^{i(kr-\pi/4)} \left(1 + \frac{3i}{8kr}\right) - \frac{1}{k^2 r^3}, & r \gg 1/k_0, \\ \frac{1}{a + \sqrt{a^2 + r^2}} + \frac{i\pi k}{4}, & r \gg 1/k_0 \end{cases} \quad (\text{A11})$$

From Eqs. (24), (A7), and (A8) we get

$$\delta n_{\omega}^{\text{P}}(\mathbf{r}) = l^2(x - iy) \left[f'' + \frac{3f'}{r} \right], \quad (\text{A12})$$

$$\delta \mathbf{v}_{\omega}^{\text{P}}(\mathbf{r}) = \omega l^2(x - iy) \left[i \frac{(rf)'}{r} \mathbf{e}_r + \frac{f}{r} \mathbf{e}_{\varphi} \right], \quad (\text{A13})$$

$$\delta \mathbf{v}_{\omega}^{\text{D}}(\mathbf{r}) = \frac{eE_0(\mathbf{e}_x - i\mathbf{e}_y)}{2m(\gamma - i\omega)}. \quad (\text{A14})$$

As seen, velocity oscillations can be presented as a sum of the f -dependent inhomogeneous contribution and the homogeneous Drude contribution, given, respectively, by Eq. (A13) and Eq. (A14)

Appendix B: Expressions for R_i^{P} and Φ_2^{P} for a single nanosphere

Using Eqs. (A10), (A11), (A12), (A13), (A14), and (18), we find

$$R_1^{\text{P}} = -i\omega l^4 (rf'' + 3f')(rf^*)' + c.c. \approx \pi\omega l^4 \begin{cases} \frac{k_0^2}{r} e^{-Qr}, & r > 1/k_0, \\ \frac{k_0 r}{2(r^2 + a^3)^{3/2}}, & r < 1/k_0, \end{cases} \quad (\text{B1})$$

$$\Phi_1^{\text{P}} = \omega l^4 (rf'' + 3f')f^* + c.c. \approx \pi\omega l^4 \begin{cases} -\frac{k_0}{r^2} e^{-Qr}, & r > 1/k_0, \\ -\frac{2}{\pi} \frac{r}{(r^2 + a^2)^{3/2}(a + \sqrt{r^2 + a^2})}, & r < 1/k_0, \end{cases} \quad (\text{B2})$$

$$R_2^{\text{P}} = -\frac{\omega^2 l^4}{\gamma} [(rf^*)'(rf)'' + f^*f'] + c.c. \\ \approx \frac{\pi\omega^2 l^4}{\gamma} \begin{cases} \frac{k_0}{2r^2} (1 + Qr) e^{-Qr}, & r > 1/k_0, \\ \frac{2}{\pi} \frac{r}{(a + \sqrt{r^2 + a^2})^3} \left[\frac{a^3}{(a^2 + r^2)^2} + \frac{r^2 + 3a^2}{(a^2 + r^2)^{3/2}} \right], & r < 1/k_0, \end{cases} \quad (\text{B3})$$

$$\Phi_2^{\text{P}} = 0. \quad (\text{B4})$$

Appendix C: Expressions for R_i^M and Φ_i^M for a single nanosphere

By direct averaging of $\delta n^P \delta \mathbf{v}^D$ over time we get

$$R_1^M - i\Phi_1^M = \frac{2l^4 s^2}{R^3} \frac{r f'' + 3f'}{\gamma + i\omega}. \quad (C1)$$

In the limiting cases, assuming $\omega \gg \gamma$ and taking in all terms lowest non-zero order with respect to γ/ω we get

$$R_1^M = \frac{2l^4 s^2}{R^3} \begin{cases} \frac{\sqrt{\pi} k_0^{3/2} e^{-Qr/2} \cos(k_0 r + \frac{\pi}{4})}{\omega \sqrt{2r}}, & r > 1/k_0 \\ -\frac{\gamma}{\omega^2 (r^2 + a^2)^{3/2}}, & r < 1/k_0 \end{cases} \quad (C2)$$

and

$$\Phi_1^M = -\frac{2l^4 s^2}{\omega R^3} \begin{cases} \frac{\sqrt{\pi} k_0^{3/2} e^{-Qr/2} \sin(k_0 r + \frac{\pi}{4})}{\sqrt{2r}}, & r > 1/k_0 \\ \frac{r}{(r^2 + a^2)^{3/2}}, & r < 1/k_0 \end{cases} \quad (C3)$$

Finally, from Eqs. (18), (A13), and (A14) we find (in the lowest order with respect to γ/ω)

$$\begin{aligned} R_2^M &= -\frac{l^4 s^2}{\gamma R^3} (r f'' + 3f') + c.c. \\ &= \frac{2l^4 s^2}{\gamma R^3} \begin{cases} \frac{\sqrt{\pi} k_0^{3/2} e^{-Qr/2} \sin(k_0 r + \frac{\pi}{4})}{\sqrt{2r}}, & r > 1/k_0, \\ \frac{r}{(a^2 + r^2)^{3/2}}, & r < 1/k_0, \end{cases} \end{aligned} \quad (C4)$$

$$\Phi_2^M = 0. \quad (C5)$$

Appendix D: Asymptotical values of j_{dc} and E_{dc} for a single nanosphere

Using Eqs. (B1),(B2),(B3),(B4), (C2),(C3),(C4), and (C5), we find asymptotical behavior of j_{dc} and E_{dc} with account of both plasmonic and mixed contribution

$$j_{dc} = -\frac{\omega l^4 N_0}{a^3} \begin{cases} A \left(\frac{r}{a} \right) + \frac{a}{R^3 k_0^2} C \left(\frac{r}{a} \right), & r \ll 1/k_0, \\ \frac{\pi a^3}{r^3} \left[k_0 r e^{-Qr} + \sqrt{\frac{2}{\pi k_0 r}} \left(\frac{r}{R} \right)^3 e^{-Qr/2} \sin \left(k_0 r + \frac{\pi}{4} \right) \right], & 1/k_0 \ll r \ll \frac{\ln[k_0/Q]}{Q} \\ 6a^3 \left(-\frac{1}{k_0^7 r^7} + \frac{1}{R^3 k_0^4 r^4} \right), & \frac{\ln[k_0/Q]}{Q} \ll r, \end{cases} \quad (D1)$$

$$\frac{eE^{dc}}{m} = -\frac{\omega^2 l^4}{a^3} \begin{cases} \pi B\left(\frac{r}{a}\right) + \frac{a}{R^3 k_0^2} C\left(\frac{r}{a}\right), & r \ll 1/k_0, \\ \frac{\pi a^3}{r^3} \left[\frac{k_0 r}{2} e^{-Qr} + \sqrt{\frac{2}{\pi k_0 r}} \left(\frac{r}{R}\right)^3 e^{-Qr/2} \sin\left(k_0 r + \frac{\pi}{4}\right) \right], & 1/k_0 \ll r \ll \frac{\ln[k_0/Q]}{Q}, \\ 6a^3 \left(\frac{5}{k_0^7 r^7} + \frac{1}{R^3 k_0^4 r^4} \right), & \frac{\ln[k_0/Q]}{Q} \ll r, \end{cases} \quad (D2)$$

where

$$A(x) = \frac{2x}{(1+x^2)^{3/2}(1+\sqrt{1+x^2})}, \quad (D3)$$

$$B(x) = \frac{2x}{(1+\sqrt{1+x^2})^3} \frac{1+(3+x^2)\sqrt{1+x^2}}{(1+x^2)^2},$$

$$C(x) = \frac{2x}{(1+x^2)^{3/2}} \quad (D4)$$

Appendix E: Expressions for $\mathbf{J}_i^P, \mathbf{J}_i^M$ for periodic array of nanospheres.

The rectified currents \mathbf{J}_i^P are given by double sums over \mathbf{q}, \mathbf{q}' , while \mathbf{J}_i^M by ordinary ones. For convenience of further calculations, in plasmonic contribution we introduce Kronecker symbol $\delta_{\mathbf{Q}, \mathbf{q}-\mathbf{q}'}$ and sum over \mathbf{Q} :

$$\mathbf{J}_1^P(\mathbf{r}) = \sum_{\mathbf{Q}} e^{i\mathbf{Q}\mathbf{r}} \mathbf{J}_{1\mathbf{Q}}^P + c.c. = \frac{4\pi^2 l^4}{d^4} \sum_{\mathbf{Q}} e^{i\mathbf{Q}\mathbf{r}} \sum_{\mathbf{q}, \mathbf{q}'} \delta_{\mathbf{Q}, \mathbf{q}-\mathbf{q}'} \frac{e^{-i(\varphi_{\mathbf{q}} - \varphi_{\mathbf{q}'}) - a(q+q')} \omega \mathbf{q} \mathbf{q}'^2}{(q^2 - k^2)(q'^2 - k^{*2})} + c.c. \quad (E1)$$

$$\mathbf{J}_2^P(\mathbf{r}) = \sum_{\mathbf{Q}} e^{i\mathbf{Q}\mathbf{r}} \mathbf{J}_{2\mathbf{Q}}^P + c.c. = \frac{4i\pi^2 l^4}{d^4 \gamma} \sum_{\mathbf{Q}} e^{i\mathbf{Q}\mathbf{r}} \sum_{\mathbf{q}, \mathbf{q}'} \delta_{\mathbf{Q}, \mathbf{q}-\mathbf{q}'} \frac{e^{-i(\varphi_{\mathbf{q}} - \varphi_{\mathbf{q}'}) - a(q+q')} \omega^2 (\mathbf{q} \mathbf{q}') \mathbf{q}'}{(q^2 - k^2)(q'^2 - k^{*2})} + c.c. \quad (E2)$$

$$\mathbf{J}_1^M(\mathbf{r}) = \sum_{\mathbf{Q}} e^{i\mathbf{Q}\mathbf{r}} \mathbf{J}_{1\mathbf{Q}}^M + c.c. = \frac{2i\pi l^4 s^2}{d^2 R^3} \frac{1}{\gamma + i\omega} \sum_{\mathbf{Q}} \frac{e^{i\mathbf{Q}\mathbf{r} - i\varphi_{\mathbf{Q}} - aQ} Q^2}{(Q^2 - k^2)} (\mathbf{e}_x + i\mathbf{e}_y) + c.c. \quad (E3)$$

$$\mathbf{J}_2^M(\mathbf{r}) = \sum_{\mathbf{Q}} e^{i\mathbf{Q}\mathbf{r}} \mathbf{J}_{2\mathbf{Q}}^M + c.c. = \frac{2\pi l^4 s^2}{d^2 R^3 \gamma} \frac{1}{\gamma + i\omega} \sum_{\mathbf{Q}} \frac{e^{i\mathbf{Q}\mathbf{r}} e^{-aQ} \omega \mathbf{Q} \mathbf{Q}}{Q^2 - k^2} + h.c. \quad (E4)$$

Using Eqs. (31) and (32) we find expression for optically-induced dc current, which includes both plasmonic and mixed contributions:

$$\mathbf{j}^{dc} = N_0 \frac{4\pi^2 l^4}{d^4} \left\{ \omega \sum_{\mathbf{q}, \mathbf{q}'} \frac{[\mathbf{e}_z \times (\mathbf{q} - \mathbf{q}')] \cdot \left(\frac{[\mathbf{e}_z \times (\mathbf{q} - \mathbf{q}')] \mathbf{q}}{|\mathbf{q} - \mathbf{q}'|} \right)}{|\mathbf{q} - \mathbf{q}'|} \frac{q'^2 e^{i(\mathbf{q}-\mathbf{q}')\mathbf{r}} e^{-i(\varphi_{\mathbf{q}} - \varphi_{\mathbf{q}'}) - a(q+q')}}{(q^2 - k^2)(q'^2 - k^{*2})} \right. \\ \left. + \frac{is^2 d^2}{2\pi R^3} \frac{1}{\gamma + i\omega} \sum_{\mathbf{Q}} \frac{[\mathbf{e}_z \times \mathbf{Q}] \cdot \left(\frac{[\mathbf{e}_z \times \mathbf{Q}] (\mathbf{e}_x + i\mathbf{e}_y)}{Q} \right)}{Q} \frac{Q^2 e^{i\mathbf{Q}\mathbf{r} - i\varphi_{\mathbf{Q}} - aQ}}{Q^2 - k^2} \right\} + c.c. \quad (E5)$$

$$\frac{e\mathbf{E}_{dc}}{m} = \gamma \sum_{\mathbf{Q}} \frac{\mathbf{Q}}{Q} \left\{ \frac{\mathbf{Q}}{Q} [\mathbf{J}_{1\mathbf{Q}}^{\text{P}} + \mathbf{J}_{2\mathbf{Q}}^{\text{P}} + \mathbf{J}_{1\mathbf{Q}}^{\text{M}} + \mathbf{J}_{2\mathbf{Q}}^{\text{M}}] \right\} e^{i\mathbf{Q}\mathbf{r}} + c.c. \quad (\text{E6})$$

$$\approx (\text{for } \gamma \ll \omega) \approx \gamma \sum_{\mathbf{Q}} \frac{\mathbf{Q}}{Q} \left\{ \frac{\mathbf{Q}}{Q} [\mathbf{J}_{2\mathbf{Q}}^{\text{P}} + \mathbf{J}_{2\mathbf{Q}}^{\text{M}}] \right\} e^{i\mathbf{Q}\mathbf{r}} + c.c. \quad (\text{E7})$$

$$= \frac{4\pi^2 l^4}{d^4} \left\{ i\omega^2 \sum_{\mathbf{q}, \mathbf{q}'} \frac{\mathbf{q} - \mathbf{q}'}{|\mathbf{q} - \mathbf{q}'|} \left[\frac{(\mathbf{q} - \mathbf{q}')\mathbf{q}'}{|\mathbf{q} - \mathbf{q}'|} \right] \frac{(\mathbf{q}\mathbf{q}')e^{i(\mathbf{q}-\mathbf{q}')\mathbf{r}} e^{-i(\varphi_{\mathbf{q}} - \varphi_{\mathbf{q}'}) - a(q+q')}}{(q^2 - k^2)(q'^2 - k^{*2})} \right. \\ \left. - i \frac{s^2 d^2}{2\pi R^3} \sum_{\mathbf{Q}} \frac{Q\mathbf{Q}e^{i\mathbf{Q}\mathbf{r} - aQ}}{Q^2 - k^2} \right\} + c.c. \quad (\text{E8})$$

Appendix F: Expressions for rectified currents in the fundamental plasmonic mode

For $(n, m) = (1, 0), (0, 1), (-1, 0), (0, -1)$, we have $q = q_0 = 2\pi/d$. Simple calculations yield

$$\mathbf{J}_1^{\text{P}} = \frac{32\pi^2 l^4}{d^4} \frac{\omega q_0^3 [\sin(q_0 y) \cos(q_0 x) \mathbf{e}_x - \sin(q_0 x) \cos(q_0 y) \mathbf{e}_y]}{|q_0^2 - k^2|^2} e^{-2q_0 a}, \quad (\text{F1})$$

$$\mathbf{J}_2^{\text{P}} = \frac{32\pi^2 l^4}{d^4} \frac{\omega^2 q_0^3 [\sin(q_0 x) \cos(q_0 x) \mathbf{e}_x + \sin(q_0 y) \cos(q_0 y) \mathbf{e}_y]}{\gamma |q_0^2 - k^2|^2} e^{-2q_0 a}, \quad (\text{F2})$$

$$\mathbf{J}_1^{\text{M}} = \frac{4\pi l^4}{d^2 R^3} \frac{q_0^2 \omega}{k_*^2 (q_0^2 - k^2)} [i \sin(q_0 x) + \sin(q_0 y)] (\mathbf{e}_x + i\mathbf{e}_y) e^{-q_0 a} + c.c. \quad (\text{F3})$$

$$\mathbf{J}_2^{\text{M}} = \frac{4\pi l^4}{d^2 R^3} \frac{q_0^2 \omega^2}{\gamma k_*^2 (q_0^2 - k^2)} [\sin(q_0 x) \mathbf{e}_x + \sin(q_0 y) \mathbf{e}_y] e^{-q_0 a} + c.c. \quad (\text{F4})$$

Next, we substitute these equations into Eqs. (32) and (33). The latter can be written in the operator form

$$\mathbf{j}_{dc} = N_0 \frac{-\nabla \text{div} + \Delta}{\Delta} (\mathbf{J}_1^{\text{P}} + \mathbf{J}_1^{\text{M}}), \quad (\text{F5})$$

$$\frac{e\mathbf{E}_{dc}}{m} = \gamma \frac{\nabla}{\Delta} \text{div} (\mathbf{J}_1^{\text{P}} + \mathbf{J}_1^{\text{M}} + \mathbf{J}_2^{\text{P}} + \mathbf{J}_2^{\text{M}}), \quad (\text{F6})$$

$$\frac{e\phi_{dc}}{m} = \gamma \frac{1}{\Delta} \text{div} (\mathbf{J}_1^{\text{P}} + \mathbf{J}_1^{\text{M}} + \mathbf{J}_2^{\text{P}} + \mathbf{J}_2^{\text{M}}). \quad (\text{F7})$$

From Eqs. (F1), (F2), (F3), (F4), (F5), (F6), and (F7), we find

$$\mathbf{j}_{dc} = N_0 \left\{ \frac{16\pi^2 l^4}{d^4} \frac{\omega q_0^3 e^{-2q_0 a} [\sin(q_0 y) \cos(q_0 x) \mathbf{e}_x - \sin(q_0 x) \cos(q_0 y) \mathbf{e}_y]}{|q_0^2 - k^2|^2} \right. \\ \left. + \frac{4\pi l^4}{d^2 R^3} \frac{\omega q_0^2 e^{-q_0 a} [\sin(q_0 y) \mathbf{e}_x - \sin(q_0 x) \mathbf{e}_y]}{k_*^2 (q_0^2 - k^2)} \right\} + c.c. \quad (\text{F8})$$

Close to resonance, this equation can be simplified and written in the form Eq. (22) with $\boldsymbol{\pi}$ and $\boldsymbol{\mu}$

given by Eq. (39) and (40), respectively. We also find (for $\gamma \ll \omega$)

$$\frac{e\mathbf{E}_{\text{dc}}}{m} = \left\{ \frac{16\pi^2 l^4 \omega^2 q_0^3 e^{-2q_0 a} [\sin(q_0 x) \cos(q_0 x) \mathbf{e}_x + \sin(q_0 y) \cos(q_0 y) \mathbf{e}_y]}{d^4 |q_0^2 - k^2|^2} + \frac{4\pi l^4 \omega^2 q_0^2 e^{-q_0 a} [\sin(q_0 x) \mathbf{e}_x + \sin(q_0 y) \mathbf{e}_y]}{d^2 R^3 k_*^2 (q_0^2 - k^2)} \right\} + c.c., \quad (\text{F9})$$

$$\frac{e\phi_{\text{dc}}}{m} = \left\{ \frac{4\pi^2 l^4 \omega^2 q_0^2 e^{-2q_0 a} [\cos(2q_0 x) + \cos(2q_0 y)]}{d^4 |q_0^2 - k^2|^2} + \frac{4\pi l^4 \omega^2 q_0 e^{-q_0 a} [\cos(q_0 x) + \cos(q_0 y)]}{d^2 R^3 k_*^2 (q_0^2 - k^2)} \right\} + c.c. \quad (\text{F10})$$

-
- [1] L. P. Pitaevskii, Sov. Phys. JETP **12**, 1008 (1961).
- [2] J. P. van der Ziel, P. S. Pershan and L. D. Malmstrom, Phys. Rev. Lett. **15**, 190 (1965).
- [3] A. V. Kimel, A. Kirilyuk, P. A. Usachev, R. V. Pisarev, A. M. Balbashov and Th. Rasing, Nature **435**, 655 (2005).
- [4] A. Kirilyuk, A. V. Kimel, and T. Rasing, Rev. Mod. Phys. **82**, 2731 (2010).
- [5] A. Kirilyuk, A. V. Kimel and Th. Rasing, Phil. Trans. R. Soc. A **369**, 3631 (2011).
- [6] O. V. Kibis, Phys. Rev. Lett. **107**, 106802 (2011).
- [7] O. V. Kibis, O. Kyriienko, I. A. Shelykh, Phys. Rev. B **87**, 245437 (2013).
- [8] A. M. Alexeev, I. A. Shelykh, M. E. Portnoi, Phys. Rev. B **88**, 085429 (2013).
- [9] F. K. Joibari, Ya. M. Blanter, G. E. W. Bauer, Phys. Rev. B **90**, 155301 (2014).
- [10] A. M. Alexeev, M. E. Portnoi, Phys. Rev. B **85**, 245419 (2012).
- [11] V. V. Kruglyak, M. E. Portnoi, Technical Physics Letters, **31**, 1047 (2005) [Pisma v Zh. Tekh. Fiziki **31**, 20 (2005)].
- [12] V. V. Kruglyak, M. E. Portnoi, R. J. Hicken, Journal of Nanophotonics, **1**, 013502 (2007).
- [13] M. L. Polianski, Phys. Rev. B **80**, 241301(R) (2009).
- [14] K. L. Koshelev, V. Yu. Kachorovskii, and M. Titov, Phys. Rev. B **92**, 235426 (2015).
- [15] K. L. Koshelev, V. Yu. Kachorovskii, M. Titov, and M. S. Shur, Phys. Rev. B **95**, 035418 (2017).
- [16] M. I. Dyakonov and M. S. Shur, Phys. Rev. Lett. **71**, 2465 (1993).
- [17] E. L. Ivchenko and S. D. Ganichev, Pisma v ZheTF **93**, 752 (2011) [JETP Lett. **93**, 673 (2011)].
- [18] J. B. Khurgin, Nature Nanotechnology **10**, 2 (2015).
- [19] P. Nordlander, Nature Nanotechnology **8**, 76 (2013).
- [20] J. Heber, Nature Materials **11**, 745 (2012).
- [21] A. N. Grigorenko, M. Polini, K. S. Novoselov, Nature Photonics **6**, 749 (2012).
- [22] F. H. L. Koppens, D. E. Chang, F. J. Garcia de Abajo, Nano Lett. **11**, 3370 (2011).
- [23] D. K. Gramotnev and S. I. Bozhevolnyi, Nature Photonics **4**, 83 (2010).
- [24] S. A. Maier, *Plasmonics: Fundamentals and Applications* (Springer, 2007).
- [25] R. N. Gurzhi, Usp. Fiz. Nauk **94**, 689 (1968) [Sov. Phys. Usp. **11**, 255 (1968)].
- [26] M. J. M. de Jong, L. W. Molenkamp, Phys. Rev. B **51**, 13389 (1985).
- [27] M. I. Dyakonov and M. S. Shur, Phys. Rev. B **51**, 14341 (1995).
- [28] M. I. Dyakonov and M. S. Shur, IEEE Trans. on Elec. Dev. **43**, 380 (1996).
- [29] A. P. Dmitriev, A. S. Furman, and V. Yu. Kachorovskii, Phys. Rev. B **54**, 14020 (1996).
- [30] A. P. Dmitriev, A. S. Furman, V. Yu. Kachorovskii, G. G. Samsonidze, and Ge. G. Sam-

- sonidze, Phys. Rev. B **55**, 10319 (1997).
- [31] T. Otsuji and M.S. Shur, IEEE Microwave Magazine, **15**, 43 (2014).
- [32] W. Knap, D. B. But, N. Dyakonova, D. Coquillat, A. Gutin, O. Klimenko, S. Blin, F. Tepe, M. S. Shur, T. Nagatsuma, S. D. Ganichev, and T. Otsuji, *Recent Results on Broadband Nanotransistor Based THz Detectors* in NATO Science for Peace and Security Series B, Physics and Biophysics: THz and Security Applications, edited by C. Corsi, F. Sizov, (Springer, Dordrecht, Netherlands, 2014).
- [33] R. Jaggi, J. Appl. Phys. **69**, 816 (1991).
- [34] R. N. Gurzhi, A. N. Kalinenko, and A. I. Kopeliovich, Phys. Rev. Lett. **72**, 3872 (1995).
- [35] K. Damle, S. Sachdev, Phys. Rev. B **56**, 8714 (1997).
- [36] H. Buhmann, L. W. Molenkamp, R. N. Gurzhi, A. N. Kalinenko, A. I. Kopeliovich and A. V. Yanovsky, Low Temp. Phys. **24**, 737 (1998).
- [37] H. Predel, H. Buhmann, L. W. Molenkamp, R. N. Gurzhi, A. N. Kalinenko, A. I. Kopeliovich, and A. V. Yanovsky, Phys. Rev. B **62**, 2057 (2000).
- [38] A. V. Andreev, S. A. Kivelson, and B. Spivak, Phys. Rev. Lett. **106**, 256804 (2011).
- [39] D. Forcella, J. Zaanen, D. Valentini, and D. van der Marel, Phys. Rev. B **90**, 035143 (2014).
- [40] A. Tomadin, G. Vignale, and M. Polini, Phys. Rev. Lett. **113**, 235901 (2014).
- [41] P. S. Alekseev, Phys. Rev. Lett. **117**, 166601 (2016)
- [42] A. B. Kashuba, Phys. Rev. B **78**, 085415 (2008).
- [43] L. Fritz, J. Schmalian, M. Müller, and S. Sachdev, Phys. Rev. B **78**, 085416 (2008).
- [44] M. Müller, J. Schmalian, and L. Fritz, Phys. Rev. Lett. **103**, 025301 (2009).
- [45] M. Mendoza, H. J. Herrmann, and S. Succi, Phys. Rev. Lett. **106**, 156601 (2011).
- [46] B. N. Narozhny, I. V. Gornyi, M. Titov, M. Schütt, and A. D. Mirlin, Phys. Rev. B **91**, 035414 (2015).
- [47] A. Cortijo, Y. Ferreirós, K. Landsteiner, and M. A. H. Vozmediano, Phys. Rev. Lett. **115**, 177202 (2015).
- [48] L. Levitov, G. Falkovich, Nat. Phys. **12**, 672 (2016).
- [49] G. Falkovich and L. Levitov, Phys. Rev. Lett. **119**, 066601 (2017).
- [50] S. Danz and B. N. Narozhny (2019), arXiv:1910.1447
- [51] H.-Y. Xie and A. Levchenko, Phys. Rev. B **99**, 045434 (2019).
- [52] S. Danz, M. Titov, B. N. Narozhny (2019), arXiv:1912.12341
- [53] This equation interpolates between asymptotes at $r \gg a$, where one can put $a = 0$ and the case $r \ll 1/|k|$, where one can use expansion over k up to the first order with the parametrical matching at $a \ll r \ll 1/|k|$.